

Rib formation in the fracture of polymethyl methacrylate

R. P. KUSY, H. B. LEE, D. T. TURNER

Dental Research Center, University of North Carolina at Chapel Hill, North Carolina, USA

Polymethyl methacrylate was fractured under a variety of loading conditions. Various linear features were observed on fracture surfaces but attention was centered on ribs of torn-out material. Such ribs were formed only in cases where loading conditions resulted in a tensile stress field ahead of the crack tip. Moreover the width of the ribs, and also their spacing, increased as the crack traversed the specimen into zones of increasing tensile stress. These observations, along with previously published data on the dependence of rib spacing on molecular weight and temperature, led to the conclusion that rib formation was due to secondary tensile fractures. These were identified to be showers of microcracks, from side views of the ribs. Fractographic evidence was obtained that the crack accelerates after formation of each rib (i.e. shower) and a "stick-slip" mechanism adopted.

1. Introduction

Zandman studied the fracture of polymethyl methacrylate (PMMA) under a variety of loading conditions and reported a correspondingly wide variety of surface features [1]. Subsequently, following Newman and Wolock [2], attention was confined mainly to specimens fractured by simple tension, presumably because this seemed to offer the simplest approach towards more detailed interpretation of fracture surface morphology. Reversing this trend, the present work is concerned with observations made under a variety of loading conditions. However, in order to avoid a discursive catalogue of observations attention will be centred on the formation of "rib" markings. Ribs appear as lines on the fracture surface disposed perpendicularly to the direction of crack propagation. Microscopic examination shows them to comprise rough regions described as due to "ruptures par arrachement" [1] or "fracture by pulling-out" [2]. Generally, ribs are found to alternate, more or less regularly, with relatively smooth regions leading to the concept of a "rib spacing" [1, 2].

Periodic markings are observed on fracture surfaces of other glassy polymers but their relationship to rib formation in PMMA is not clear.

118

Polystyrene has been investigated in most detail and a mechanism proposed to account for a "band" structure [3]. It has been suggested that this mechanism applies to other glassy polymers, but not to high molecular weight PMMA [4]. The present work is confined to PMMA of high molecular weight, i.e. $> 10^5$.

2. Experimental

Commercial samples of cast sheets of high molecular weight PMMA were studied ("Plexiglas", Rohm

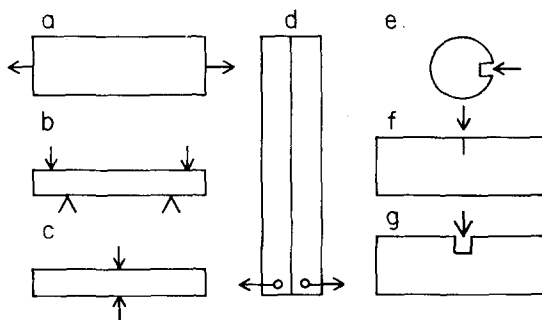


Figure 1 Schematic representation of loading conditions. a, tension; b, bending; c, clipping; d, double cantilever beam; e, wedge; f, razor impact; g, chisel impact. The double cantilever beam specimen includes two surface slots represented by the solid line.

and Haas Company, Philadelphia). Viscosity average molecular weights, M , were calculated from limiting viscosity numbers determined in benzene at 25° C [5].

Specimens were loaded to fracture at ambient temperature (22° C) and humidity (30%). Slots were cut with a saw. They were pulled in simple tension using an Instron machine (Fig. 1a), bent by hand (b), and clipped with hand cutters (c). Double cantilever beam specimens, with sides slotted to guide crack growth [6], were tested on an Instron machine (d). A steel wedge was driven by hand screw against the sides of a slot in a disc (e) [7]. A razor blade was held in a slot in the side of a specimen and struck with a hammer (f). In a similar impact experiment a blunt chisel was used (g).

Fracture surfaces were examined by reflected light (bright field) using a Zeiss Universal Microscope. Rib spacings were determined with a travelling microscope.

3. Results

An overview of the types of fracture surfaces observed is indicated in Fig. 2. In order to help put the significance and limitations of these schematics in perspective, a collage of a fracture surface formed by tension is shown for comparison (Fig. 3). This exhibits a relatively smooth "mirror" region followed by a "mist" region which is densely covered by conic sections, predominantly parabolas, which have diagnostic value because they point away from the direction of crack growth. In the schematic only a few parabolas are indicated. On the fracture surface the first few ribs

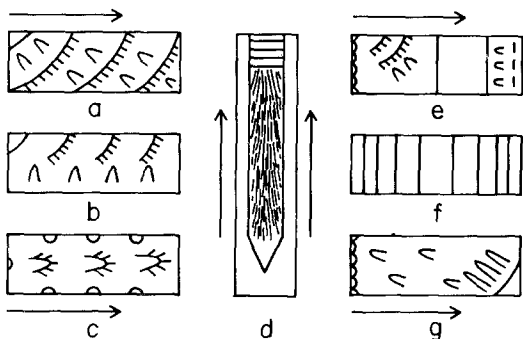


Figure 2 Schematic representation of fracture surfaces. The arrows represent the direction of crack propagation with respect to the ribs (|||||) and miscellaneous linear features (——). The parabolas point away from the direction of local crack propagation. The broken line in surface (e) represents crack arrest.

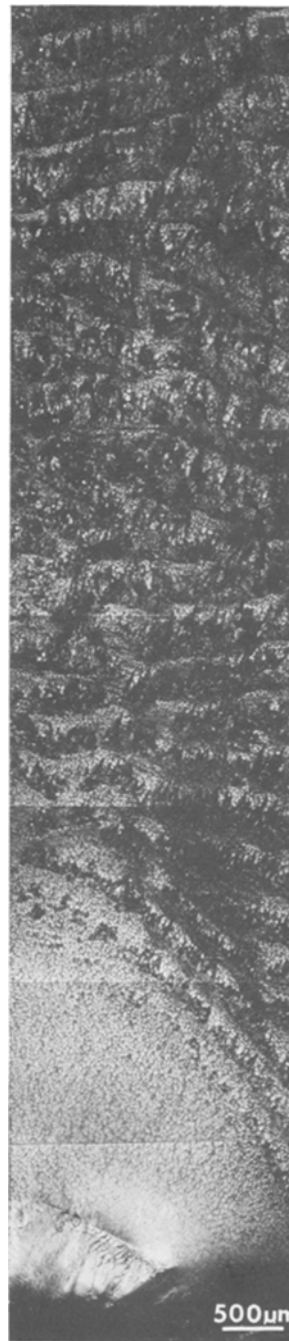


Figure 3 Fracture surface after tensile failure. Specimen 7.0 cm \times 1.25 cm \times 0.25 cm; nominal slot depth = 0.1 cm; $M = 5.4 \times 10^5$.

are seen as incomplete dark (rough) features while all the lighter (smoother) features include conic markings. Because of their similar appearance, the smooth features may be regarded as extensions of the mist region. The ribs eventually lose their initial symmetry with respect to the boundary of the mirror region. In the schematic only the first

few ribs are indicated, as though continuous features, with small secondary lines representing more or less irregular extensions of the rough parts of the ribs into the smooth parts, cf. Fig. 3. The simple lines, without secondary fracture markings (Fig. 2d to g), are intended to represent any other extensive linear features other than ribs. In fact, these features vary considerably in microscopic detail and will present a challenge for future study.

3.1. Simple tension

3.1.1. Influence of slot depth

Specimens broken without artificial surface flaws generally exhibit only a limited number of ribs adjacent to the mist region, the remainder of the fracture surface being too rough and irregular to allow clear definition by optical microscopy. With slots of increasing depth the area of the mist region increases as does the area of clear resolution of the ribs (Fig. 4). The spacing between ribs closest to the mirror is about $300\ \mu\text{m}$. However, with decreasing slot depth the spacing increases with distance from the mirror up to as much as

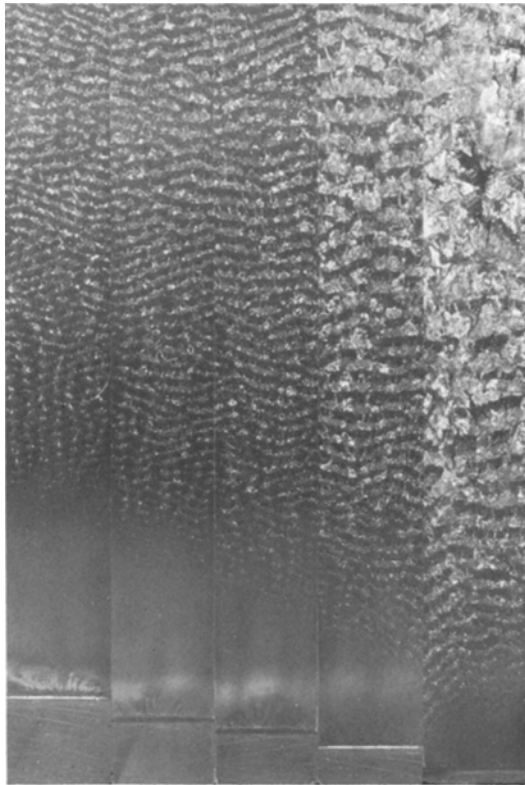


Figure 4 Influence of slot depth on fracture after tensile failure. Specimen $12.7\ \text{cm} \times 2.5\ \text{cm} \times 0.3\ \text{cm}$; nominal slot depths from right to left: 0.05, 0.10, 0.15, 0.20 and 0.25 cm; $M = 8.9 \times 10^6$.

$1300\ \mu\text{m}$. The increase in the length of the rough portion of the rib, which corresponds to the lighter parts in Fig. 4, is particularly marked.

Notching was stated by Zandman to have an effect on rib spacing but details were not given [1]. A statement, by Andrews, that "the spacing increases with distance from the origin" [8] is consistent with the present results.

3.1.2. Influence of rate of loading

Zandman found that at very low rates of loading, taking several months before fracture, the mirror region occupies the whole fracture surface. With increasing rate of loading in the range 0.1 to $500\ \text{kg mm}^{-2}\ \text{h}^{-1}$, it was shown that both mirror and mist regions decreased in area. However, the spacing between ribs was not affected. In the present work these findings were confirmed and extended using a specimen with the following characteristics, dimensions $6.6\ \text{cm} \times 1.0\ \text{cm} \times 0.2\ \text{cm}$, slot depth = $0.2\ \text{cm}$, $M = 1.1 \times 10^6$. In this case rib spacing was measured close to the mist region.

TABLE I Influence of rate of loading on average rib spacing

	Load rate ($\text{kg mm}^{-2}\ \text{h}^{-1}$)			
	4×10^1	4×10^2	4×10^3	4×10^4
Rib spacing (μm)	380	340	340	380

3.2. Bending

Specimens fractured by bending form ribs only along the side placed in tension prior to fracture. The disposition of the parabolic markings shows that the crack propagates along the edge of the specimen and then turns towards the side originally in compression (cf. Fig. 2b).

Although the ribs are incomplete, in the sense that they do not extend from one edge of the fracture surface to the other, each one is more continuous than ribs formed in simple tension. This more orderly arrangement facilitates measurement of the spacing between adjacent ribs with increasing distance away from the origin of fracture. The spacing between ribs at the beginning of the mist region is about $300\ \mu\text{m}$ and increases to about $700\ \mu\text{m}$ at the end of the specimen. Introduction of a slot prior to fracture greatly reduces this increase in spacing (Fig. 5). These results are similar to those described above for simple tension experiments.

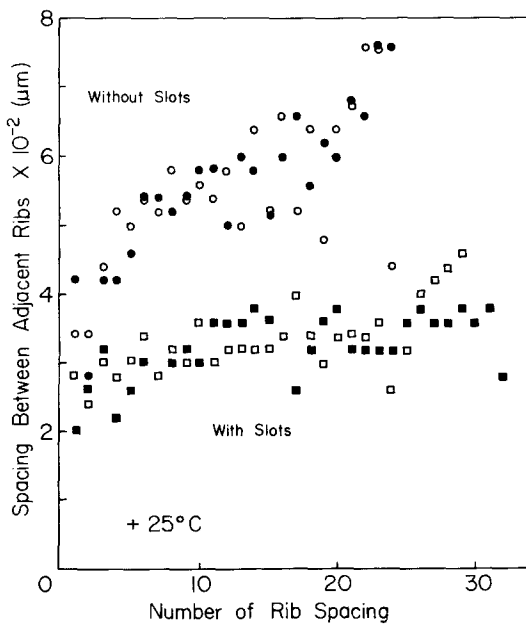


Figure 5 Spacing between adjacent ribs after bending failure. Specimen 8 cm \times 2 cm \times 0.25 cm; $M = 1.1 \times 10^6$. Successive spacings are numbered from end of mist region to end of specimen. Key: ●, ○ – no slot (two specimens); □ – slot = 1 mm; ■ – slot = 3 mm.

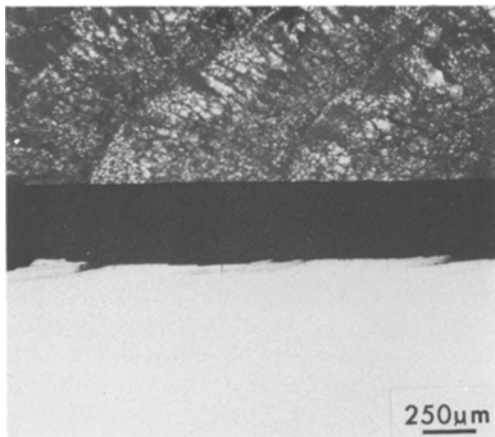


Figure 6 Relationship between ribs and markings on adjacent side after bending failure. As the three fracture showers indicate, fracture proceeded from right to left.

Examination of the side adjacent to a fracture surface reveals the markings shown in Fig. 6. Similar markings are also observable in specimens fractured by simple tension but are, generally, less distinct. Evidence that these markings are associated with the rough portion of the rib is obtained by matching views of the fracture surface with its adjacent side (Fig. 6).

3.3. Clipping

Clipping is expected to cause compression of both surface zones with corresponding tension near the middle of the specimen. The ribs are formed in the zone which was in tension prior to fracture and the parabolic markings indicate that the crack turns towards both surfaces (Fig. 2c). An interesting feature of this mode of fracture is that the spacing between adjacent ribs, although varying erratically between about 200 and 400 μm ($M = 1.1 \times 10^6$), does not increase with distance from the mirror as observed in the cases of simple tension and bending.

3.4. Double cantilever beam

The double cantilever beam has commanded interest as a means of effecting cleavage at a controlled slow rate of crack propagation (of the order 0.1 cm sec⁻¹). Attention has been given to the measurement of the work required to generate a fracture surface and the appearance of the fracture surface. In PMMA, at 20°C, “river patterns” with green and red interference colors were reported [6]. Similar effects were noted in the present work.

As the crack approaches the end of the beam it accelerates and generates a series of features, perpendicular to the direction of crack propagation, which appear as faint “lines” (Fig. 2d). On magnification these features are seen to increase in width towards the end of the specimen (Fig. 7a and b); they are irregularly spaced.

3.5. Wedge loading

When a wedge is driven into a slot, in a disc of PMMA, a stress builds up. If the procedure is slow (> 15 sec) an optical distortion, due to flow, is seen to occur at the tip of the slot and a crack eventually takes off at an angle to the plane of the slot. This generally gives an irregular surface inconvenient for microscopic study. If the procedure is faster (< 10 sec) distortion is limited and a crack suddenly takes off in the plane of the slot and, with the geometry of specimen used (diameter = 2.5 cm, thickness = 0.25 cm, slot = 0.5 cm \times 0.1 cm), is arrested after traversing most of the diameter. In the schematic illustration (Fig. 2e) the arrest is indicated by a broken line. The appearance of the fracture surface may include all the following features indicated in the illustration: first, a series of small mirror regions near the tip of the slot; second, a few ribs with a spacing of about

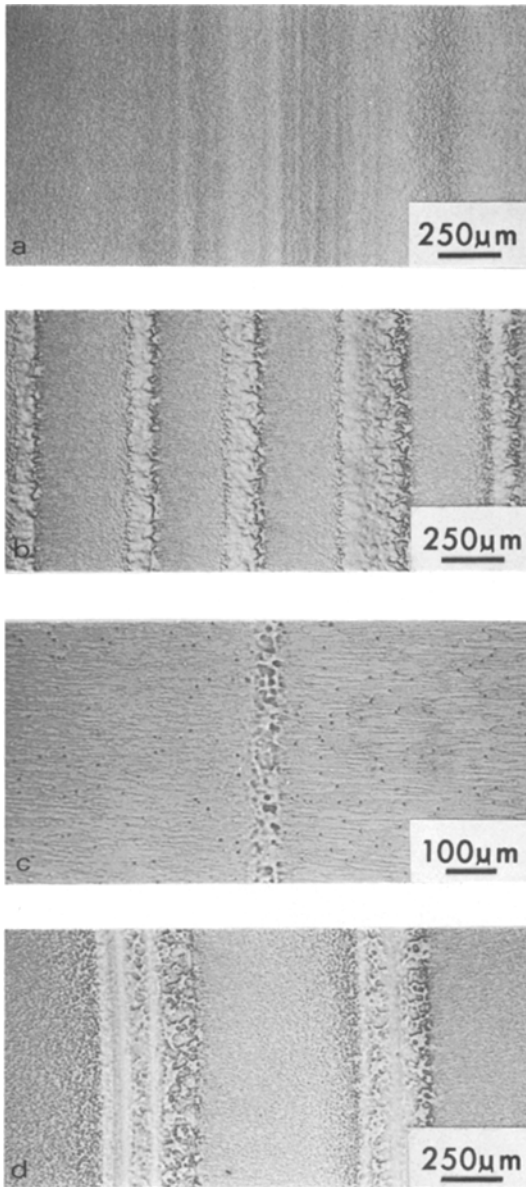


Figure 7 Appearance of linear features. Fracture proceeded from left to right. (a) and (b) Features observed at end of cantilever beam in region generated during crack acceleration ($M = 2.9 \times 10^6$). (c) Feature formed by wedge loading (e) ($M = 1.1 \times 10^6$). (d) Features formed by razor impact (f) ($M = 1.1 \times 10^6$).

200 μm ; third, parabolas in a mist region; fourth, an intense single linear feature; and finally, a weaker linear feature (Fig. 7c) followed by elongated parabolic markings. The remainder of the surface is irrelevant because it was formed by snapping the small portion of the specimen left intact after crack arrest.

3.6. Razor impact

Striking a razor into a slot (size not critical) results in a smooth surface with lines which appear red on a green background. The spacing of the lines is irregular but in many instances they appear to be more widely separated near the center of the specimen (Fig. 2f). On magnification, most of the "lines" are seen to be single bands but occasionally multiple bands are observed (Fig. 7d).

3.7. Chisel impact

At the region of impact multiple mirrors are often seen which are succeeded by a mist which covers most of the fracture surface. The definition of the parabolas in this dull brown mist region is unusually sharp. Near the end of the surface the parabolas increase in length and intense interference colours appear. This is followed by a bright featureless region bounded by a single "line" (Fig. 2g).

4. Discussion

A mechanism of rib formation should take account of the following observations and conclusions:

(1) A rib is the locus of intersection of microcracks which may be seen under the microscope along with occasional protruding features. These protrusions are adjacent to the microcracks and appear to have been torn from them. They are not shown in the present work because of the limited depth of focus in optical microscopy. A more detailed study would be pursued more effectively by scanning electron microscopy.

(2) A side view of a rib shows it to be comprised of a family of microcracks mostly originating from a localized region on, or near, the fracture surface. Previously a distinction between crack bifurcation, observed in PMMA, and formation of numerous cracks, observed in nylon, has been made by George and the latter phenomenon designated as a "fracture shower" [9]. This designation will be adopted to describe the present observations.

(3) In simple tension, rib spacing is independent of rate of loading at least within a range stated above. As noted by Zandman at a very low rate, approaching creep, specimens may be fractured without rib formation.

(4) When specimens are fractured under a variety of loading conditions ribs are formed only when a tensile stress field pre-existed ahead of the

crack tip, i.e. before crack propagation. This restriction obviously applies in the bending and clipping modes of fracture (Fig. 1b and c). In cleavage tests, which are designed to localize a tensile stress at the tip of the crack, no ribs are formed. Even when the crack accelerates, the excess energy, over the minimal requirement to form fracture surfaces, is expended with formation of features other than ribs (Fig. 2d).

(5) Rib spacing may increase, by a factor of about three, with increasing distance from the site of crack initiation. The increase is greatly reduced if fracture is initiated from a slot. The increase is not observed as a result of clipping.

(6) The increase in rib spacing is mainly due to an increase in width of the ribs themselves. The intermediate mist regions are, relatively, unaffected (Fig. 4).

(7) The intermediate mist regions include conic sections, parabolas, etc. Their observed decrease in size provides evidence that the crack again accelerates after formation of each rib. This type of evidence has been deduced previously, for example with respect to similar observations concerning the "band" structure on fracture surfaces of polystyrene [3].

(8) Finally, two important observations must be included which were made in previous work on PMMA. First, it has been reported [2], and confirmed [10], that rib spacing decreases with molecular weight. For example, the spacing is $350\ \mu\text{m}$ for a viscosity average molecular weight of 5.4×10^5 and decreases to $3\ \mu\text{m}$ when the molecular weight is degraded by γ -irradiation to 2.5×10^4 [10]. It should be noted that the fracture surface changes in appearance for molecular weight $\lesssim 10^5$ and, hence, the present comments apply to polymers of high molecular weight, i.e. $\geq 10^5$.

(9) The second observation from previous work is that rib spacing was found, in bending, to decrease by a factor of less than three in the temperature range of from $+77$ to -196°C [11].

In order to account for the observations that a tensile stress field must exist for ribs to form, (3) and (4), and the dependence of ribs on molecular weight, (8), and temperature, (9), it is postulated that ribs are caused by secondary tensile fractures. The evidence for this is that tensile strength, which is related to the primary fracture which results in separation of the specimen into pieces, is analogously sensitive to changes in molecular weight and also relatively insensitive to

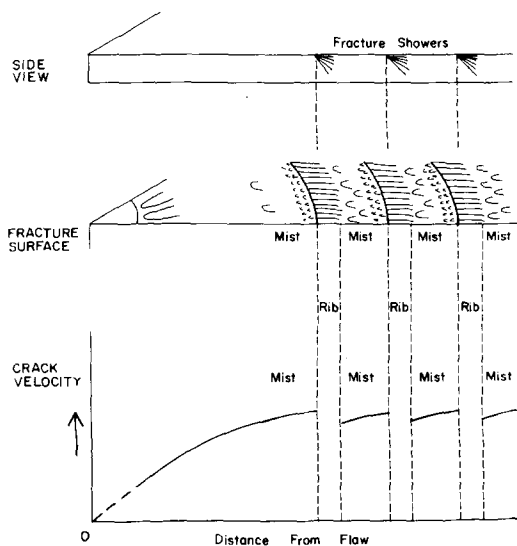


Figure 8 Relationship between ribs and associated secondary fracture showers with crack velocity. The size and symmetry of the showers is exaggerated, cf. Fig. 6.

temperature [8]. By direct observation, the mode of secondary tensile fracture is "shower" formation. The relationship between ribs and showers, (1) and (2), is represented schematically in Fig. 8.

The alternation of ribs with smoother, mist, regions was first noted by Zandman. He suggested that the fracture propagates "in jumps" with each rib corresponding to an "arrest". This suggestion was based on photoelastic evidence of fluctuations in stress during fracture. However, the influence on rib formation was not considered in detail and an alternative, more explicit, relationship with respect to crack velocity is preferred (Fig. 8). The general form of the dependence of crack velocity on path length has been determined directly for PMMA over a range of strain-rates, which bracket those under consideration in the present work [12]. The experimental technique used, depending on the breaking of electrically conducting paths, was too insensitive to detect changes of velocity in path lengths as short as a few hundred μm , as postulated in Fig. 8. Only indirect evidence for fluctuations in velocity is available from the interpretation of fractographic markings (7). However, background support for the idea can be deduced from Yoffe's theoretical analysis showing that a crack in an elastic material is expected to accelerate to a limiting velocity and then branch [13]. This branching would be expected to relieve stress and hence decelerate the crack [8]. If, as in the present experiments, the stress is restored, then

the processes of crack acceleration and branching would be repeated generating a sequence of branching sites, i.e. a sequence of ribs.

While the first few ribs in Fig. 8 are represented as approximately equivalent, in fact the width of each subsequent rib, and consequently the rib spacing, increases in simple tensile and bending tests, (5) and (6). An explanation can be offered from Smekal's work that, as a crack cleaves through a specimen subjected to uniaxial extension, the strain energy increases as the load bearing cross-section diminishes ahead of the crack tip [14]. Smekal developed this idea to account for secondary fracture markings initiated ahead of the crack tip in inorganic glasses. In a general way, this idea could be extended to account for increasingly violent branching and hence wider ribs. The effect would be diminished by reducing the accumulation of stress by use of stress concentrations, such as slots, and would not be favoured under the localized loading of clipping.

In broader perspective the above mechanism can be classified as "stick-slip". It is similar to a suggestion made by Andrews involving "sticking" resulting from crack bifurcation [8]. It differs, however, in being consistent with the present observed morphology of the ribs. In contrast, Andrews' mechanism predicts the formation of "surface mounds" (see [8]). It would be interesting to check whether or not this morphology corresponds to some other surface feature noted in the present work which has been neglected since it is not a rib. A second classification of mechanisms attributes a major role to stress waves as a contributory factor to surface morphology. Stress waves are known to be of importance in accounting for Wallner lines observed on the fracture surfaces of inorganic glasses [14]. A case has also been made that they are important in explaining patterns generated in natural rubber, compounded with carbon black, when fractured below its glass transition temperature [15].

Recently, Green and Platt have claimed that rib formation in PMMA "has been identified as a Wallner-line phenomenon". This claim is based on a comparison of a theoretical construct of the locus of intersection of stress waves and crack fronts, having a reasonable ratio of velocities of about 2, and the geometrical disposition of individual experimentally observed ribs [16]. However, the claim of an identity appears to be too strong because a number of arbitrary decisions are in-

volved which give considerable latitude in arriving at a fit between theory and experiment. One of these decisions involves an arbitrary choice of a spatial point source for the emission of stress waves. Another arbitrary choice is in the selection of particular ribs for comparison from arrays which may vary in disposition in ways which have not been demonstrated to be reproducible in the detail predicted by the theoretical construct. Because of reservations of this kind, the present attitude is to suspend judgement concerning the role of stress waves in rib markings in PMMA of high molecular weight. However, evidence that stress waves may assume importance at lower molecular weights ($< 10^5$) will be reported subsequently [10].

Acknowledgements

This investigation was supported by NIH research grant number DE 02668 from the National Institute of Dental Research and by NIH grant number RR 05333 from the Division of Research Facilities and Resources. Partial support was obtained from the Materials Research Center, University of North Carolina, under Grant No. GH 33632 from the National Science Foundation.

References

1. F. ZANDMAN, "Études de la Déformation et de la Ruptures des Matières Plastiques", (Publications Scientifiques et Techniques de Ministère de l'Air, Paris, 1954).
2. S. B. NEWMAN and I. WOLOCK, *J. Appl. Phys.* **29** (1958) 49.
3. M. J. DOYLE, A. MANCINI, E. OROWAN and S. T. STORK, *Proc. Roy. Soc.* **A329** (1972) 137.
4. M. J. DOYLE, *J. Mater. Sci.* **10** (1975) 159.
5. J. BRANDRUP and E. H. IMMERGUT, eds., "Polymer Handbook", Part IV (Interscience, New York, 1967).
6. L. J. BROUTMAN and F. J. MCGARRY, *J. Appl. Polymer Sci.* **9** (1965) 589.
7. H. D. MOSCOWITZ and D. T. TURNER, *J. Mater. Sci.* **9** (1974) 861.
8. E. H. ANDREWS, "Fracture in Polymers" (Oliver and Boyd, Edinburgh, 1968).
9. W. GEORGE, *Ind. Eng. Chem.* **44** (1952) 1328.
10. R. P. KUSY and D. T. TURNER, unpublished work.
11. R. P. KUSY, H. B. LEE and D. T. TURNER, unpublished work.
12. A. KOBAYASHI, N. OHTANI and T. SATO, *J. Appl. Polymer Sci.* **18** (1974) 1625.
13. E. H. YOFFE, *Phil. Mag.* **42** (1951) 739.
14. A. SMEKAL, *Ergeb. exakt. Naturw.* **15** (1936) 106.
15. E. H. ANDREWS, *J. Appl. Phys.* **30** (1959) 740.
16. A. K. GREEN and P. L. PLATT, *Eng. Fracture Mech.* **6** (1974) 71.

Received 31 March and accepted 23 June 1975.